Evaluation of Paper-based Loop-Mediated Isothermal Amplification

Taehong Kim[a], Gopal Palla[b], Bibek Raut[b], Mohit S. Verma[b,c,d,**], Arezoo M. Ardekani[a,*]

[a]*School of Mechanical Engineering, Purdue University, West Lafayette, 47907, Indiana, United States*
[b]*Department of Agricultural & Biological Engineering, Purdue University, West Lafayette, 47907, Indiana, United States*
[c]*Birck Nanotechnology Center, Purdue University, West Lafayette, 47907, Indiana, United States*
[d]*Weldon School of Biomedical Engineering, Purdue University, West Lafayette, 47907, Indiana, United States*

Abstract

Paper-based loop-mediated isothermal amplification (LAMP) platforms have garnered increasing attention as an alternative to conventional liquid-phase systems, owing to their inherent portability, low-cost fabrication, and user-friendly operation. However, the reaction of paper-based LAMP can be slower than that of liquid-based LAMP. Enhancing the reaction rate in these devices requires a multidisciplinary understanding of heat transfer, diffusion in porous substrates, and nonspecific interaction of reactants with the paper. In this study, heat transfer within both systems is modeled numerically, and effective diffusion within the paper is discussed. Additionally, we demonstrate that pre-treating the paper with bovine serum albumin (BSA) effectively blocks nonspecific binding sites, resulting in an acceleration of amplification of the synthetic gene of the orf7ab of SARS-CoV-2 (NC_045512.2) by approximately 7 minutes. This work presents a quantitative framework for evaluating amplification efficiency in paper-based nucleic acid diagnostics and introduces a straightforward, low-cost strategy for enhancing their performance.

Keywords: Loop-Mediated Isothermal Amplification (LAMP); Paper-based Devices; Nucleic Acid Amplification Technologies (NAAT); Diffusion in Paper; Heat transfer in Paper; Nonspecific Binding

1. Introduction

During and after the COVID-19 pandemic, one of the most highlighted technologies is nucleic acid amplification technologies (NAATs), including Loop-mediated isothermal amplification (LAMP),[1, 2, 3] which is a powerful nucleic acid amplification method that achieves high sensitivity and specificity under isothermal temperature conditions.[4, 5, 6] Another NAAT, quantitative reverse-transcription polymerase chain reaction (RT-qPCR) has been established as the gold standard detection technique for various viruses.[7] However, the need for sample extraction and purification limits field deployability and leads to long processing times.[8] The long processing time has been a critical drawback of the test since it is not suitable

*Corresponding author: ardekani@purdue.edu
**Co-corresponding author: msverma@purdue.edu

for preventing the spread of the disease. The field deployability of RT-qPCR is limited too, due to its low portability and difficulty of use.[9, 10] These drawbacks are from the inevitable temperature cycling for denaturation of the produced DNA in each cycle.

LAMP offers advantages in field deployability and ease of use. It is faster than RT-qPCR and simplifies the process by eliminating the need for temperature cycling through the use of primers that form loops. It prevents the formation of double-stranded DNA (dsDNA), thereby eliminating the need for the denaturation step, which is required at each cycle in qPCR.[4, 5, 11] Additionally, colorimetric indicators can visualize LAMP results visually, eliminating the need for specialized fluorescence readers. These qualities make RT-LAMP particularly more suitable for point-of-care devices than RT-qPCR.[12, 13, 14, 15, 16, 17]

Given its sensitivity and minimal equipment needs, RT-LAMP has been successfully implemented on paper-based analytical devices for portable diagnostics,[2, 3, 13] like other portable devices.[18] Paper-based and paper-polymer hybrid RT-LAMP platforms combine biochemical amplification with microfluidic paper channels, having gained attention as alternative platforms because they offer excellent compatibility with nucleic acids and proteins, are simple to manage with reduced volume per reaction, and are cost-effective to produce. [19, 20] As a result, various biomolecules such as Zika virus,[21, 22] bacterial DNA,[23] Foodborne pathogen,[24, 25, 26, 27] rotavirus A.[28] have been successfully detected by paper-based RT-LAMP devices. However, adapting an isothermal amplification to a paper matrix poses unique engineering challenges, such as non-uniform color changes across a paper device. Among these challenges, the paper-based LAMP reaction is known to have a slower reaction than liquid-based LAMP, which is one of key parameters as well as specificity and sensitivity.[2]

Although research has been conducted to scrutinize the dynamics of the LAMP reaction,[29] dynamics of the paper-based LAMP reaction have not been thoroughly investigated. In this study, we evaluate the performance of LAMP in a paper-based device compared to a liquid-based (tube-based) LAMP assay. We specifically investigate the extent of heat transfer limitations, diffusion constraints, and the impact of surface adsorption on the efficiency and speed of amplification in the paper platform. We show that the reduced diffusion in the paper-based device and the nonspecific binding (NSB) of reactants to the cellulose matrix are the main causes of reduced reaction speed in the paper-based assay. In addition, we suggest an example solution for reducing NSB by using blocking agents, as well as the importance of the timing of agent application. The findings inform the design of a more efficient, portable paper-based LAMP device by minimizing NSB and enhancing effective diffusion through the selection of high-porosity paper.

2. Materials and methods

2.1. Fabrication of the paper-based device

The paper device consists of a serial array of 3 mm × 3 mm × 1.1 mm (length (l) × width (w) × height (h)) paper pads and 2 mm × 3 mm × 0.5mm (l×w×h) polystyrene spacers (Tekra Double White opaque HIPS Polystyrene Litho Grade).[3] The Ahlstrom chromatography electrophoresis and blotting paper, grade 222, is used. It is cut by a cutting machine (Xhixumm electric leather cutting machine) and is fixed with

Components	Concentration	Remarks
KCl	62.5 mM	
$MgSO_4$	10 mM	
dNTPs	1.75 mM	
Bst 2.0	807 mU/μL	
Phenol red	0.125 mM	
dUTPs	0.175 mM	
Antartic Thermolabile UDG	0.25 mU/μL	
Tween 20	1.25%	
Primer mix	12.5%	
Betaine	25 mM	
Trehalose	18%	
BSA	0.626 μg/μL	excluded in ”other reactants”

Table 1: Composition of Master mix. BSA is excluded when it is mentioned as ”other reactants” in this article.

adhesive film (Tekra Melinex 454 polyester). Then, the strips with the paper pads are encapsulated in a 1.5 mm thick laser-cut Acrylic frame and a PCR adhesive film.[17]

2.2. LAMP reaction

Homemade master mix was used. The master mix is composed as shown in Table 1. Six primers for the orf7ab.1 of SARS-CoV-2 (NC_045512.2) were utilized like previous work[2]: FIP(5’-GGA GAG TAA AGT TCT TGA ACT TCC TAG TTA CGT AGA TCA G-3’), BIP(5’-TGC GGC AAT AGT GTT TAT AAC ACT ATG AAA GTT CAA TCA TTC TGT CT-3’), LF(5’-TGT CTG ATG AAC AGT TTA GGT GAA A-3’), LB(5’-TTG CTT CAC ACT CAA AAG AA-3’), F3(5’-CGG CGT AAA ACA CGT CTA-3’), B3(5’-GCT AAA AAG CAC AAA TAG AAG TC-3’). The primer mix has 16 μM FIP, 16 μM BIP, 4 μM LF, 4 μM LB, 2 μM F3, and 2 μM B3. In the liquid-based LAMP, 7.5 μL of template is added to 17.5 μL of reaction mix, resulting in a total solution volume of 25 μL. In the paper-based LAMP, 7.5 μL of mixed solution of the master mix and template is used in one reaction for the experiment to compare paper-based LAMP and liquid-based LAMP. For another experiment, having control of different pre-treatments of the reaction, some chemicals were dried overnight (24 hours) in room temperature (RT) to ensure the liquid volume in the paper device did not exceed the device’s capacity. A commercial heater (Anova precision cooker) is used to heat the water baths for liquid-based LAMP and paper-based LAMP.

2.3. Quantification of hue

For paper-based devices, timelapse images were captured at 20-30 second intervals using a flatbed scanner at 600 dpi resolution (Epson Perfection V850 Pro Scanner).[30] For liquid-based devices, the timelapse images are captured at 20-30 second intervals by a homemade device having a CMOS camera with LED

backlights, and the hue is extracted from homemade software. Images were processed with a Python script, a home-made code to extract the hue.[17] The measured hues were normalized by subtracting the hue obtained at the start, and the net hue change was obtained for each colorimetric LAMP reaction.

2.4. SARS-CoV-2 Artificial synthetic gene

We purchased the SARS-COV-2 orf7ab (NC_045512.2) synthetic gene from GenScript. The whole sequence is: ATG AAA ATT ATT CTT TTC TTG GCA CTG ATA ACA CTC GCT ACT TGT GAG CTT TAT CAC TAC CAA GAG TGT GTT AGA GGT ACA ACA GTA CTT TTA AAA GAA CCT TGC TCT TCT GGA ACA TAC GAG GGC AAT TCA CCA TTT CAT CCT CTA GCT GAT AAC AAA TTT GCA CTG ACT TGC TTT AGC ACT CAA TTT GCT TTT GCT TGT CCT GAC GGC GTA AAA CAC GTC TAT CAG TTA CGT GCC AGA TCA GTT TCA CCT AAA CTG TTC ATC AGA CAA GAG GAA GTT CAA GAA CTT TAC TCT CCA ATT TTT CTT ATT GTT GCG GCA ATA GTG TTT ATA ACA CTT TGC TTC ACA CTC AAA AGA AAG ACA GAA TGA TTG AAC TTT CAT TAA TTG ACT TCT ATT TGT GCT TTT TAG CCT TTC TGC TAT TCC TTG TTT TAA TTA TGC TTA TTA TCT TTT GGT TCT CAC TTG AAC TGC AAG ATC ATA ATG AAA CTT GTC ACG CCT AAA.

2.5. Calculation of Time-to-threshold (Tt)

Net hues were extracted from time-lapse colorimetric images of LAMP reactions. Each amplification curve represents the evolution of net hues over 60 minutes. No Template Controls (NTC) were included in each assay batch to define the reaction threshold. Prior to analysis, a 5-point moving average was followed by Gaussian smoothing with a window size of 2, equivalent to a standard deviation of approximately 2. Amplification curves were classified as positive or negative using an NTC-derived threshold. The final hue at 60 minutes from all NTCs was used to calculate a threshold as:

$$\text{Threshold} = \mu_{\text{NTC}} + 4 \times \sigma_{\text{NTC}}$$

where μ_{NTC} and σ_{NTC} denote the mean and standard deviation of the final NTC hue values, respectively. The constant 4 was arbitrarily defined to help differentiate between positive and negative reactions. Only curves exceeding this threshold were processed further for Time-to-threshold (Tt) analysis. The Tt value is defined as the time it takes for the curve to overcome the threshold.

3. Results and Discussion

As shown in Figure 1, the LAMP reaction time is evaluated by measuring the hue change over time. Figure 1a shows an example picture of PCR tubes submerged in a water bath. The same reaction mix is used in liquid-based LAMP and paper-based LAMP, as shown in Table 1. The same number of genomic copies is added in both cases, which are 10^3, 10^4, 10^5, and 10^6 genomic copies per reaction. From Figure 1a, the left three samples in the bottom row are when the genomic copies are 10^6 per reaction, and the three samples next to them are when the genomic copies are 10^5 per reaction. The top left three samples are when

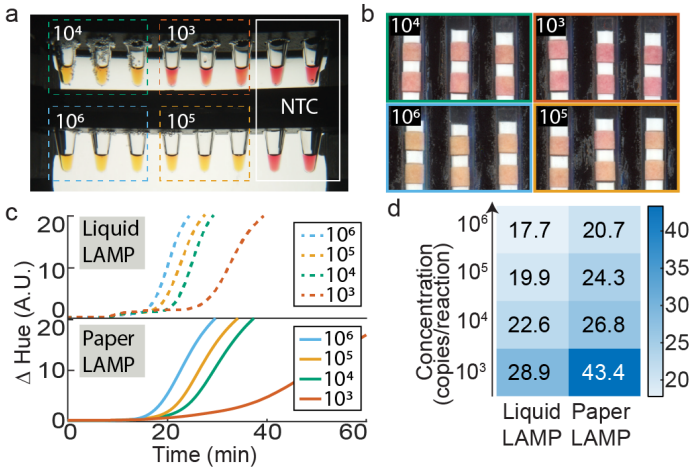

Figure 1: LAMP time differences between liquid-based LAMP and paper-based LAMP. (a) Experimental setup for liquid-based LAMP. (b) Experimental setup of paper-based LAMP. (c) Net hue changes over time of liquid-based LAMP (Top) and paper-based LAMP (Bottom). (d) A heatmap of Tts of liquid-based LAMP and paper-based LAMP with various concentrations

the genomic copies are 10^4, and the three samples next to them are when it is 10^3 per reaction. The two samples at the bottom right and the two samples at the top right are NTCs. The image is captured 30 minutes after the reaction begins. The hues of the highest genomic copies, 10^6 copies/reaction, are fully changed to yellow, while others are not yet fully changed.

In contrast, paper-based LAMP shows that the hues are not fully changed yet for the highest genomic copies, 10^6 per reaction, as shown in six paper pads in the bottom left of Figure 1b. The bottom right, the top left, and the top right are when the genomic copies are 10^5, 10^4, and 10^3 per reaction, respectively. Like Figure 1a, Figure 1b is captured 30 minutes after the reaction starts. Both liquid-based LAMP and paper-based LAMP are submerged in a 65°C water bath.

The reaction rates can be quantified by calculating the Tt value from the hue difference versus time curve, shown in Figure 1c. The y-axis in this graph represents the change in hue over time from the initial hue at the begining of the reaction. In Figure 1c, the top subfigure shows the change of the hue with respect to reaction time for liquid-based LAMP (dashed line), and the bottom subfigure shows that for paper-based LAMP (solid line). The color of the curve represents different genomic copies, 10^6, 10^5, 10^4, and 10^3, with skyblue, orange, green, and brown, respectively. For liquid-based LAMP, the curves show averages of three replicates for each genomic concentration. For paper-based LAMP, averages of six replicates are used. The calculated Tt values are visualized as a heatmap in Figure 1d. Paper-based LAMPs show Tt values of 20.7, 24.3, 26.8, and 43.4 for each concentration, 10^6, 10^5, 10^4, and 10^3 genomic copies/reaction, respectively, while the liquid-based LAMPs have Tt values of 17.7, 19.9, 22.6, and 28.9. The paper-based LAMPs are 17%, 22%, 19%, and 50% slower than liquid-based LAMPs for each concentration, 10^6, 10^5, 10^4, and 10^3 genomic copies/reaction, respectively. There is a clear lag when the LAMP is performed on paper, and it

increases with decreasing genomic copies per reaction.

Evaluating the reason for the lag in paper-based LAMP should be done from an interdisciplinary perspective by analyzing the different steps in the LAMP reaction. The LAMP reaction begins with the denaturation of dsDNA, which is triggered by the thermal breathing of the dsDNA. Dangerfield *et al.* concluded that the strand invasion during the initiation is the rate-limiting step for the LAMP reaction.[29] Then, the polymerase binding and primer binding will be done, followed by DNA synthesis by the polymerase attached to the template, which is a chemical reaction related to the concentration of the reactants near the site of reaction. Our primary focus is on heat transfer, diffusion, and NSB in a paper-based LAMP device. This is because the initial stage of the LAMP reaction, along with other reactions, heavily relies on the temperature of the sample. To assess the other reaction steps, we also evaluate the effective diffusion coefficient, which affects the reduction in the likelihood of the polymerase and primer attaching to the target. This reduction is one of the root causes of the reduced chance of reactions. Lastly, we also consider NSB of the reagents on the fibers, which will reduce the effective concentration of the reactants.

3.1. Heat transfer evaluation and effective diffusion

Unlike PCR, LAMP does not begin with a high-temperature denaturation step; instead, primer binding and strand-displacement synthesis occur concurrently at the reaction temperature. Amplification is initiated when the primers invade double-stranded DNA regions via the sporadic thermal "breathing" of the helix at the operating temperature (63–65°C).[31] This strand invasion/annealing step is known to be the rate-limiting step in LAMP kinetics.[29] This is because DNA remains largely double-stranded without sporadic breathing of double-stranded templates at low temperatures. Dangerfield *et al.* demonstrated that strand invasion, which initiates LAMP, is the rate-limiting step and becomes more efficient only as the temperature nears 65°C, where DNA duplex "breathing" increases. Jeon *et al.* showed that local denaturation ("bubble" formation) in dsDNA below the melting temperature is a thermally driven process that becomes significantly more probable as temperature approaches the critical temperature, reinforcing that efficient primer access requires a high-temperature environment [31].

The heat transfer of liquid-based LAMP has an advantage due to convection within the tube and the absence of an air pocket, unlike paper-based LAMP. However, it has a disadvantage due to a larger heating fluid volume compared to paper-based LAMP, at 25 μL and 7.5 μL, respectively. We conducted a numerical study to investigate the heat transfer of the paper-based LAMP device submerged in a water bath and the PCR tube-based LAMP in the bath. Blue and orange solid lines in Figure 2a represent the average temperature of the paper and the PCR tube, respectively. The paper device and PCR tube are surrounded by 65°C water. Regarding the paper device, the plastic cartridge and the air pocket above the paper device are also implemented. The heat transfer of a water-filled PCR tube in a water bath is simulated within a two-dimensional axisymmetric domain, as shown in Figures 2c. As shown in Figure 2a, 25 μL samples reach 63°C in under 49 seconds in liquid-based LAMP. In contrast, paper-based LAMP may take longer to reach the same temperature, 77 seconds. However, the time gap between the heat transfer of the water-filled PCR tube and that of the paper-based device is not significant. The difference in heat transfer (28 seconds) does

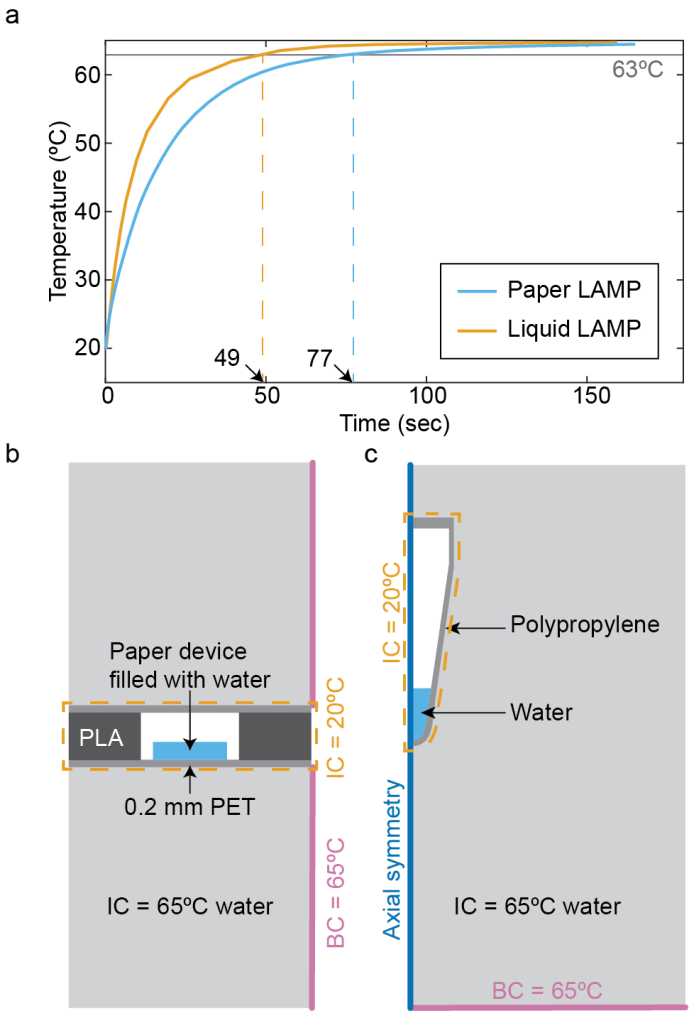

Figure 2: Numerical study of heat transfer. (a) Temperature with respect to time. (b) Simulation domain of the paper-based LAMP. (c) Simulation domain of the liquid-based LAMP

Thickness (θ)	Basis Weight (w)	Density of cotton fiber (ρ_{cotton})
0.81 mm	0.302 kg/m^2	1500 kg/m^3

Table 2: Properties of the Ahlstrom chromatography electrophoresis and blotting paper grade 222.

not fully explain the initial question, the difference between the liquid-based LAMP and the paper-based LAMP (up to 15 minutes).

After denaturation, the reaction depends on either the reaction rate or the diffusion rate, whichever is slower. For qualitative comparison, the Damköhler number (Da) can be calculated. Da is a dimensionless number used to compare the reaction rate to the transport rate in a chemical system. The general term of a first-order reaction is that $Da = kL^2/D$, where k is the reaction rate constant, L is the characteristic length, and D is the diffusion coefficient. Given that the D of DNA and polymerase is in order 10^{-10} m^2/s,[32, 33] k is of the order of 100 s^{-1},[29] the characteristic length of the paper device is approximately 1 cm, the Da is on the order of 10^8, indicating that the reaction rate is much faster than the diffusion rate. This implies that the overall process is diffusion-limited, meaning that the transport of reactants to the active sites governs the overall reaction speed in the device.

The diffusion can be affected by the fibers in the paper. Effective diffusion is a term used to describe reduced diffusion due to obstacles in the matrix, a phenomenon that has been extensively researched by various researchers. One of the most well-known equations of effective diffusion in saturated porous media is defined as $D_e = \frac{\varepsilon}{\tau}D$, where ε is porosity, τ is the diffusive tortuosity, and D is the diffusion coefficient, respectively. The diffusive tortuosity is defined as $\tau = (< L_d > /L_s)^2$ where $< L_d >$ is the average length of a chemical's diffusive pathway and L_s is the straight-line length.[34] The tortuosity factor accounts for the reduced diffusivity because the solid grains impede Brownian motion. For saturated porous media, the Weissberg model, $\tau = 1 - 0.5 \ln \varepsilon$, or the Archie model, $\tau = \varepsilon^{-\beta}$, are commonly used, where β is a constant which can be found experimentally.[34, 35, 36] As examples of the Archie model, the Millington and Quirk model is $\tau = \varepsilon^{-1/3}$,[37] and the Delgado model uses $\tau = \varepsilon^{-0.4}$.[38] We can qualitatively estimate the reduced diffusion, even though tortuosity is not a function of porosity alone, so the constants of these equations cannot be universal and require evaluation.

According to the manufacturer's information, the properties of the paper we used are shown in Table 2.[39] The ε value of the paper, 75%, can be calculated using the formula $\varepsilon = 1 - (w/\theta)/\rho_{cotton}$, where w is the basis weight, θ is the thickness, and ρ_{cotton} is the density of cotton fiber. The effective diffusion calculated from the three models, the Weissberg model, the Millington and Quirk model, and the Delgado model, is approximately two-thirds of the diffusion coefficient without paper fibers. Since the reaction rate is proportional to the diffusion coefficient in a diffusion-limited reaction,[40, 41] the reduced diffusion in the paper device results in a 1.5 times longer reaction in the paper-based LAMP than in the liquid-based LAMP. This explains our experimental results that paper-based LAMP of the lowest genomic copies, 10^3, takes 1.5 times longer than liquid-based LAMP. In conclusion, the paper device has its inherent drawbacks due to the reduced diffusion in porous media. One solution is to use a material with higher porosity; however, there is

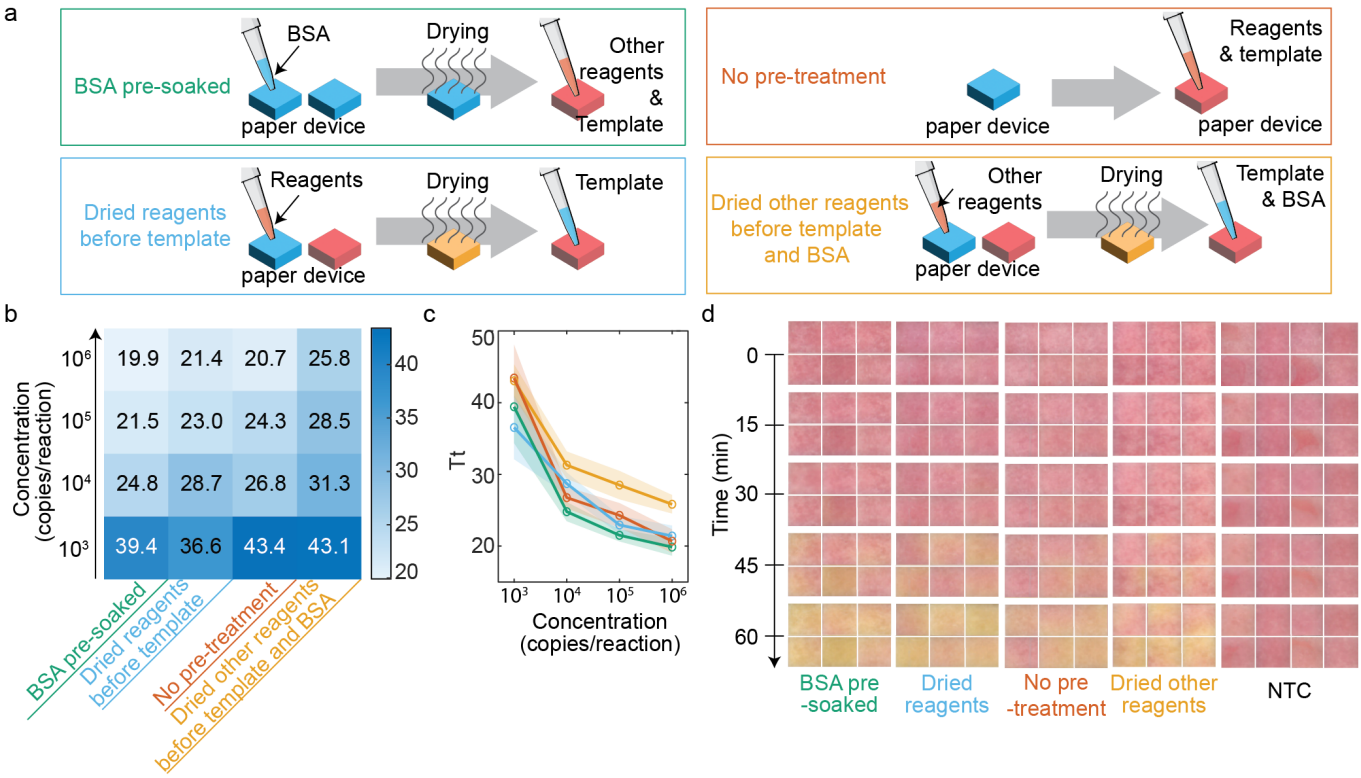

Figure 3: Experimental setup and result of the experiment with different preparations of samples. (a) Four different preparation methods for controls. The left top shows the preparation procedure for the BSA pre-soaked device. The left bottom shows the device with dried reagents before template application, the right top indicates the device without pre-treatment, while the right bottom shows dried other reagents except BSA before applying templates and BSA. (b) Heatmap of the Tt value versus genomic copies. (c) Tt for the concentration of viral copies per reaction. Shades are the standard deviation of the measurement. (d) The scanned image of paper devices with different protocols, and with respect to time. The concentration is 10^3 copies/reaction.

a limitation to increasing the porosity.

3.2. NSB of reactants on fibers in the paper device

Another possible improvement point of the lagged LAMP reaction in the paper device is reducing NSB of reactants on the fiber. Cellulose fibers can adsorb DNA, enzymes, and other reagents, thereby reducing their available concentration and inhibiting the reaction, which in turn lowers the effective reagent concentrations. It is important to reduce NSB to increase the reaction speed and sensitivity.[42] For this purpose, researchers have utilized BSA as a blocker, allowing it to occupy the NSB sites before the reaction. Previous work on paper-based LAMP also utilized BSA to improve the reaction and stabilize the reactants.[2] However, the NSB sites should be occupied with BSA first before the LAMP reaction, and so the timing of the application of BSA is important. In the paper-based LAMP reaction device, the impact of the application

timing of BSA has not been discussed yet.

An experiment is conducted to determine the impact and effectiveness of BSA regarding application timings. As shown in Figure 3a, we prepare four different controls, one of which is ”BSA pre-soaked.” The paper device is first filled with only 0.626 μg/μL solution of BSA and then dried overnight (24 hours) at RT. We apply the primers and other reactants, including templates, right before heating the device in a 65°C water bath for the LAMP reaction. The bottom left of Figure 3a shows ”Dried reagents before the template.” We apply all reagents, including BSA, and let them dry overnight (24 hours) at RT. The next day, we apply templates and heat the device in the same water bath. The top right of Figure 3a is ”No pre-treatment.” We apply all reagents and templates simultaneously and heat the device. The other one, at the bottom right of Figure 3a, shows ”Dried other reagents before template and BSA.” We soak all reagents except BSA in the device and let them dry overnight (24 hours) at RT. We apply the templates and BSA the next day and heat them for the reaction. Six replicates for each control and each concentration are captured, and all the paper-based devices are in one cartridge, which is submerged in a water bath at 65°C. The NTC has eight replicates, with two from each of the following controls: ”BSA pre-soaked”, ”dried reagents before the template”, ”no pre-treatment”, and ”dried reagents before the template and BSA.”

As shown in Figure 3b, a heatmap of the Tt value for the ”BSA pre-soaked” case reveals the lowest Tt value when the genomic copies are 10^4, 10^5, and 10^6 copies per reaction. For the lowest genomic copies of the template, ”Dried reagents before the template” showed the shortest Tt, which is slightly shorter than the ”BSA pre-soaked” case. The ”no pre-treatment” case yields results similar to those of ”Dried reagents before template” at high genomic copy numbers, such as 10^4, 10^5, and 10^6 copies per reaction. However, when the genomic copies are 10^3 copies per reaction, it surges so that the difference with the ”Dried reagents before template” case (blue label in Figure 3b) becomes 6.8 minutes. The last case, ”Dried other reagents before template and BSA,” shows the highest Tt for all concentrations.

Figure 3c shows Tt versus genomic copy concentration. When the concentration decreases, Tt value increases, and this increase is more pronounced at the lowest concentration. This is because the lowest genomic copies are almost at the edge of the limit of detection of the device, 1500 genomic copies/reaction [2]. In other words, the lowest concentration is the most focused sample among all the samples, as it represents the harshest condition for the LAMP reaction. Figure 3d shows scanned images of the paper devices when the genomic copies are 10^3 copies/reaction. The ”BSA pre-soaked”, ”Dried reagents”, ”No pre-treatment”, ”Dried other reagents”, and ”NTC” are presented from left to right, respectively. For NTC, each column shows the addition of NTC to ”BSA pre-soaked”, ”Dried reagents”, ”No pre-treatment”, and ”Dried other reagents” devices, from left to right, respectively. The scanned images are collected every fifteen minutes from the beginning to 60 minutes. For 45 min and 60 min, ”BSA pre-soaked” and ”dried reagents before template” yield a more yellowish result than the others, indicating faster reactions for them compared with the others.

From Figure 3, we can conclude that the BSA application before the reaction is beneficial, while the effect of the BSA reduces when it is applied at the same time as templates and other reactants. The application timing of BSA is a crucial factor in this experiment, as the BSA concentration (0.626 μg/μL) is identical

for all samples. This is because the BSA cannot effectively block NSB sites when it is applied with or after chemicals that need to be blocked for a faster reaction. Moreover, the ”dried other reagents before template and BSA” case shows the worst reaction speed across every concentration range, indicating that the NSB of other reagents on the paper could not be blocked by belated BSA application.

The results suggest that the aging effect is not a dominant factor and can be effectively mitigated by incorporating either ”BSA pre-soaked” or ”Dried reagents before the template.” Based on the premise that the freshness of reactants enhances reaction efficiency, it is reasonable to expect that the ”no pre-treatment” condition—where none of the reactants were subjected to one day of aging at RT—would outperform the others. However, our findings did not support this expectation.

4. Conclusion

This research explains the lag of the LAMP reaction when it happens in paper devices. Understanding the limitations and areas for improvement of the paper-based LAMP is crucial, as it offers several advantages over liquid-based LAMP, including higher mobility, ease of storage, ease of use, and reduced reaction volume. Based on the consideration of the LAMP reaction sequence, reduced heat transfer, reduced diffusivity due to the fiber structure, and NSB on the fiber are the main reasons for the lagged reaction.

We numerically evaluated the heat transfer of the device and calculated the effective diffusion coefficient, which can affect the reaction rate. There is a 30-second delay responsible for the heat transfer of the device. The diffusion is a bottleneck of the reaction rather than the chemical reaction rate. The effective diffusion coefficient was two-thirds of the original diffusion coefficient without the paper structure, resulting in up to 50% delayed reactions at 10^3 genomic copies per reaction.

Another improvement point we tackle is reducing NSB. By saturating the paper fibers with BSA before the assay, we effectively mitigated the loss of reagents to the surface. For the best result, BSA should be applied before the reaction. Although it is 10 minutes slower than the liquid-based LAMP at 10^3 genomic copies per reaction, the paper-based RT-LAMP showed a marked improvement in amplification efficiency with pre-treatment of BSA. The difference in Tt value of ”no pre-treatment” and ”Dried reactants before template” is around 5 minutes.

The paper-based LAMP device is gaining popularity due to its advantages over the liquid-based LAMP reaction. This research sheds light on the importance of diffusion and NSB on the reaction speed. Additionally, we suggest pre-coating BSA as one effective way to reduce NSB. The result can be used to design a more effective portable paper-based LAMP device by reducing NSB and enhancing the porosity of the paper to increase effective diffusion, which are key parameters in the successful development of a paper-based LAMP device.

Author Contributions

Taehong Kim: conceptualization, data curation, formal analysis, investigation, methodology, software, validation, visualization, and writing - original draft. Gopal Palla: investigation, methodology, and writing

- review & editing. Bibek Raut: Data curation, methodology, software, and writing - review & editing. Mohit S. Verma: conceptualization, funding acquisition, methodology, project administration, resources, supervision, and writing - review & editing. Arezoo M. Ardekani: conceptualization, funding acquisition, project administration, investigation, methodology, resources, supervision, and writing - review & editing.

Acknowledgement

Funding for this project was provided by the American Rescue Plan Act through USDA APHIS. The findings and conclusions in this publication are those of the author(s) and should not be construed to represent any official USDA or U.S. Government determination or policy. We sincerely thank Dr. Jiangshan Wang for his valuable advice on experimental planning. We also gratefully acknowledge Cindy Peres for her training in general nucleic acid amplification techniques.

Conflicts of Interest

There are no conflicts to declare.

Author Biographies

Taehong Kim earned his Bachelor's and Master's degrees in mechanical engineering from Sogang University, Seoul, South Korea, in 2015 and 2017, respectively. Currently, he is pursuing a Ph.D. in Mechanical Engineering at Purdue University, Indiana, United States, starting in 2021. His research focuses on both experimental and theoretical aspects of microfluid dynamics, with applications in engineering and biology.

Mohit Verma is an Associate Professor within Purdue University's Department of Agricultural and Biological Engineering, as well as the Weldon School of Biomedical Engineering. Dr. Verma specializes in biosensors for probing microbiomes at the point of need. He received his B.A.Sc. in Nanotechnology Engineering in 2012 and Ph.D. in Chemical Engineering (Nanotechnology) in 2015 from the University of Waterloo, Canada. He completed a Banting Postdoctoral Fellowship with Dr. George Whitesides at Harvard University in 2017. His innovative research encompasses a wide spectrum of applications, spanning plants, animals, humans, and the environment. His laboratory pioneers field-deployable biosensors, offering swift characterization solutions for viruses, bacteria, antimicrobial resistance genes, and fungi. This transformative technology is seamlessly transitioned to commercialization through his startup, Krishi Inc.

Arezoo Ardekani is a Professor of Mechanical Engineering at Purdue University. Honored with the Presidential Early Career Award for Scientists and Engineers (PECASE) from President Obama, Arezoo has also received an NSF CAREER Award, the Arthur B. Metzner Early Career Award from the Society of Rheology, the Society of Engineering Science (SES) Young Investigator Medal, the Sigma Xi Mid-career Research Award, and is named a Purdue University Faculty Scholar. A Fellow of the American Physical Society (APS) and American Society of Mechanical Engineers and American Institute for Medical and Biological Engineering (AIMBE), Arezoo has also received the College of Engineering Faculty Excellence

Awards for Graduate Student Mentorship and Early Career Research, the Amelia Earhart Award, and the Society of Women Engineers Award. She received her Ph.D. from the University of California Irvine in 2009 and was a Shapiro Postdoctoral Fellow at MIT. Her research focuses on the active matter, biological flows, as well as complex fluids. Arezoo is an Associate Editor of ASME Applied Mechanics Review, an Editorial Advisory Board Member of the International Journal of Multiphase Flow, Journal of Non-Newtonian Fluid Mechanics, Physics of Fluids and Physical Review Fluids and a member of the American Physical Society-Division of Fluid Dynamics (DFD) Executive Committee. She was a co-chair of the 2022 APS-DFD meeting held in Indianapolis.

References

[1] T. Kang, J. Lu, T. Yu, Y. Long, G. Liu, Advances in nucleic acid amplification techniques (NAATs): COVID-19 point-of-care diagnostics as an example, Biosensors and Bioelectronics 206 (6 2022). doi:10.1016/j.bios.2022.114109.

[2] J. L. Davidson, J. Wang, M. K. Maruthamuthu, A. Dextre, A. Pascual-Garrigos, S. Mohan, S. V. S. Putikam, F. O. I. Osman, D. McChesney, J. Seville, M. S. Verma, A paper-based colorimetric molecular test for SARS-CoV-2 in saliva, Biosensors and Bioelectronics: X 9 (12 2021). doi:10.1016/j.biosx.2021.100076.

[3] J. Wang, A. Dextre, A. Pascual-Garrigos, J. Levi Davidson, M. K. Maruthamuthu, D. McChesney, J. Seville, M. S. Verma, Fabrication of a paper-based colorimetric molecular test for SARS-CoV-2, MethodsX 8 (2021) 101586. doi:10.1016/j.biosx.2021.10.
URL `https://doi.org/10.1016/j.mex.2021.101586`

[4] T. Notomi, H. Okayama, H. Masubuchi, T. Yonekawa, K. Watanabe, N. Amino, T. Hase, Loop-mediated isothermal amplification of DNA, Nucleic Acids Research 28 (12) (2000) e63–e63. doi:10.1093/nar/28.12.e63.
URL `https://doi.org/10.1093/nar/28.12.e63`

[5] K. Nagamine, T. Hase, T. Notomi, Accelerated reaction by loop-mediated isothermal amplification using loop primers, Molecular and Cellular Probes 16 (3) (2002) 223–229. doi:10.1006/MCPR.2002.0415.

[6] Y. Zhao, F. Chen, Q. Li, L. Wang, C. Fan, Isothermal Amplification of Nucleic Acids, Chemical Reviews 115 (22) (2015) 12491–12545. doi:10.1021/acs.chemrev.5b00428.

[7] B. D. Kevadiya, J. Machhi, J. Herskovitz, M. D. Oleynikov, W. R. Blomberg, N. Bajwa, D. Soni, S. Das, M. Hasan, M. Patel, A. M. Senan, S. Gorantla, J. E. McMillan, B. Edagwa, R. Eisenberg, C. B. Gurumurthy, S. P. M. Reid, C. Punyadeera, L. Chang, H. E. Gendelman, Diagnostics for SARS-CoV-2 infections, Nature Materials 20 (5) (2021) 593–605. doi:10.1038/s41563-020-00906-z.

[8] M. Yüce, E. Filiztekin, K. G. Özkaya, COVID-19 diagnosis —A review of current methods, Biosensors and Bioelectronics 172 (1 2021). doi:10.1016/j.bios.2020.112752.

[9] D. Thompson, Y. Lei, Mini review: Recent progress in RT-LAMP enabled COVID-19 detection, Sensors and Actuators Reports 2 (1) (11 2020). doi:10.1016/j.snr.2020.100017.

[10] M. N. Esbin, O. N. Whitney, S. Chong, A. Maurer, X. Darzacq, R. Tjian, Overcoming the bottleneck to widespread testing: a rapid review of nucleic acid testing approaches for COVID-19 detection, RNA 26 (2020) 771–783. doi:10.1261/rna.
URL `http://www.rnajournal.org/cgi/doi/10.1261/rna.`

[11] K. J. Moore, J. Cahill, G. Aidelberg, R. Aronoff, A. Bektaş, D. Bezdan, D. J. Butler, S. V. Chittur, M. Codyre, F. Federici, N. A. Tanner, S. W. Tighe, R. True, S. B. Ware, A. L. Wyllie, E. E. Afshin, A. Bendesky, C. B. Chang, R. I. Rosa, E. Elhaik, D. Erickson, A. S. Goldsborough, G. Grills, K. Hadasch, A. Hayden, S. Y. Her, J. A. Karl, C. H. Kim, A. J. Kriegel, T. Kunstman, Z. Landau, K. Land, B. W. Langhorst, A. B. Lindner, B. E. Mayer, L. A. McLaughlin, M. T. McLaughlin, J. Molloy, C. Mozsary, J. L. Nadler, M. D'silva, D. Ng, D. H. O'connor, J. E. Ongerth, O. Osuolale, A. Pinharanda, D. Plenker, R. Ranjan, M. Rosbash, A. Rotem, J. Segarra, S. Schürer, S. Sherrill-Mix, H. Solo-Gabriele, S. To, M. C. Vogt, A. D. Yu, C. E. Mason, Loop-Mediated Isothermal Amplification Detection of SARS-CoV-2 and Myriad Other Applications, Journal of Biomolecular Techniques 32 (3) (2021) 228–275. doi:10.7171/jbt.21-3203-017.

[12] A. Pascual-Garrigos, M. K. Maruthamuthu, A. Ault, J. L. Davidson, G. Rudakov, D. Pillai, J. Koziol, J. P. Schoonmaker, T. Johnson, M. S. Verma, On-farm colorimetric detection of Pasteurella multocida, Mannheimia haemolytica, and Histophilus somni in crude bovine nasal samples, Veterinary Research 52 (1) (2021) 126. doi:10.1186/s13567-021-00997-9.
URL `https://doi.org/10.1186/s13567-021-00997-9`

[13] J. Wang, J. Davidson, S. Kaur, A. Dextre, M. Ranjbaran, M. Kamel, S. Athalye, M. Verma, Paper-Based Biosensors for the Detection of Nucleic Acids from Pathogens, Biosensors 12 (2022) 1094. doi:10.3390/bios12121094.

[14] J. Wang, M. Ranjbaran, A. Ault, M. S. Verma, A loop-mediated isothermal amplification assay to detect Bacteroidales and assess risk of fecal contamination, Food Microbiology 110 (2023) 104173. doi:10.1016/J.FM.2022.104173.
URL `https://www.sciencedirect.com/science/article/pii/S0740002022001976`

[15] J. Wang, S. Kaur, A. Kayabasi, M. Ranjbaran, I. Rath, I. Benschikovski, B. Raut, K. Ra, N. Rafiq, M. S. Verma, A portable, easy-to-use paper-based biosensor for rapid in-field detection of fecal contamination on fresh produce farms, Biosensors and Bioelectronics 259 (2024) 116374.

doi:10.1016/J.BIOS.2024.116374.
URL https://www.sciencedirect.com/science/article/pii/S0956566324003798

[16] M. Kamel, J. L. Davidson, J. M. Schober, G. S. Fraley, M. S. Verma, A paper-based loop-mediated isothermal amplification assay for highly pathogenic avian influenza, Scientific Reports 15 (1) (2025) 12110. doi:10.1038/s41598-025-95452-6.
URL https://doi.org/10.1038/s41598-025-95452-6

[17] B. Ahmed, B. Raut, A. Pauley, J. L. Davidson, S. Yang, M. S. Verma, Development of a portable paper-based biosensor for the identification of genetically modified corn (Zea mays) and soybean (Glycine max), Biosensors and Bioelectronics 287 (2025) 117690. doi:10.1016/J.BIOS.2025.117690.
URL https://www.sciencedirect.com/science/article/pii/S0956566325005640

[18] G. Xun, S. T. Lane, V. A. Petrov, B. E. Pepa, H. Zhao, A rapid, accurate, scalable, and portable testing system for COVID-19 diagnosis, Nature Communications 12 (1) (12 2021). doi:10.1038/s41467-021-23185-x.

[19] J. C. Linnes, A. Fan, N. M. Rodriguez, B. Lemieux, H. Kong, C. M. Klapperich, Paper-based molecular diagnostic for Chlamydia trachomatis, RSC Advances 4 (80) (2014) 42245–42251. doi:10.1039/c4ra07911f.

[20] D. Das, C. W. Lin, H. S. Chuang, LAMP-Based Point-of-Care Biosensors for Rapid Pathogen Detection, Biosensors 12 (12) (12 2022). doi:10.3390/bios12121068.

[21] K. Kaarj, P. Akarapipad, J. Y. Yoon, Simpler, Faster, and Sensitive Zika Virus Assay Using Smartphone Detection of Loop-mediated Isothermal Amplification on Paper Microfluidic Chips, Scientific Reports 8 (1) (12 2018). doi:10.1038/s41598-018-30797-9.

[22] B. S. Batule, Y. Seok, M. G. Kim, Paper-based nucleic acid testing system for simple and early diagnosis of mosquito-borne RNA viruses from human serum, Biosensors and Bioelectronics 151 (2020) 111998. doi:10.1016/J.BIOS.2019.111998.

[23] S. Roy, N. F. Mohd-Naim, M. Safavieh, M. U. Ahmed, Colorimetric Nucleic Acid Detection on Paper Microchip Using Loop Mediated Isothermal Amplification and Crystal Violet Dye, ACS Sensors 2 (11) (2017) 1713–1720. doi:10.1021/acssensors.7b00671.

[24] B. Pang, K. Fu, Y. Liu, X. Ding, J. Hu, W. Wu, K. Xu, X. Song, J. Wang, Y. Mu, C. Zhao, J. Li, Development of a self-priming PDMS/paper hybrid microfluidic chip using mixed-dye-loaded loop-mediated isothermal amplification assay for multiplex foodborne pathogens detection, Analytica Chimica Acta 1040 (2018) 81–89. doi:10.1016/J.ACA.2018.07.024.

[25] T. N. D. Trinh, N. Y. Lee, A foldable isothermal amplification microdevice for fuchsin-based colorimetric detection of multiple foodborne pathogens, Lab on a Chip 19 (8) (2019) 1397–1405. doi:10.1039/c8lc01389f.

[26] K. T. L. Trinh, T. N. D. Trinh, N. Y. Lee, Fully integrated and slidable paper-embedded plastic microdevice for point-of-care testing of multiple foodborne pathogens, Biosensors and Bioelectronics 135 (2019) 120–128. doi:10.1016/j.bios.2019.04.011.

[27] M. Zhang, J. Liu, Z. Shen, Y. Liu, Y. Song, Y. Liang, Z. Li, L. Nie, Y. Fang, Y. Zhao, A newly developed paper embedded microchip based on LAMP for rapid multiple detections of foodborne pathogens, BMC Microbiology 21 (1) (12 2021). doi:10.1186/s12866-021-02223-0.

[28] X. Ye, J. Xu, L. Lu, X. Li, X. Fang, J. Kong, Equipment-free nucleic acid extraction and amplification on a simple paper disc for point-of-care diagnosis of rotavirus A, Analytica Chimica Acta 1018 (2018) 78–85. doi:10.1016/J.ACA.2018.02.068.

[29] T. L. Dangerfield, I. Paik, S. Bhadra, K. A. Johnson, A. D. Ellington, Kinetics of elementary steps in loop-mediated isothermal amplification (LAMP) show that strand invasion during initiation is rate-limiting, Nucleic Acids Research 51 (1) (2023) 488–499. doi:10.1093/nar/gkac1221.

[30] M. S. Verma, N. Rafiq, B. Raut, Field-deployable devices, systems, and methods for isothermal assay testing and kits therefore (7 2025).

[31] J. H. Jeon, W. Sung, F. H. Ree, A semiflexible chain model of local denaturation in double-stranded DNA, Journal of Chemical Physics 124 (16) (2006). doi:10.1063/1.2192774.

[32] S. Kondrat, M. N. Popescu, Brownian dynamics assessment of enhanced diffusion exhibited by 'fluctuating-dumbbell enzymes', Physical Chemistry Chemical Physics 21 (35) (2019) 18811–18815. doi:10.1039/c9cp02842k.

[33] G. L. Lukacs, P. Haggie, O. Seksek, D. Lechardeur, N. Freedman, A. S. Verkman, Size-dependent DNA mobility in cytoplasm and nucleus, Journal of Biological Chemistry 275 (3) (2000) 1625–1629. doi:10.1074/jbc.275.3.1625.

[34] B. Ghanbarian, A. G. Hunt, R. P. Ewing, M. Sahimi, Tortuosity in Porous Media: A Critical Review, Soil Science Society of America Journal 77 (5) (2013) 1461–1477. doi:10.2136/sssaj2012.0435.

[35] H. L. Weissberg, Effective Diffusion Coefficient in Porous Media, Journal of Applied Physics 34 (9) (1963) 2636–2639. doi:10.1063/1.1729783.

[36] G. E. Archie, The electrical resistivity log as an aid in determining some reservoir characteristics, SPE reprint series (2003) 9–18.

[37] R. J. Millington, J. P. Quirk, Permeability of porous solids, Trans. Faraday Soc. 57 (0) (1961) 1200–1207. doi:10.1039/TF9615701200.
URL http://dx.doi.org/10.1039/TF9615701200

[38] J. M. Delgado, A simple experimental technique to measure tortuosity in packed beds, Canadian Journal of Chemical Engineering 84 (6) (2006) 651–655. doi:10.1002/cjce.5450840603.

[39] Ahlstrom, Chromatography and Blotting Transfers, high quality cotton paper (2023).
URL https://ahlstrom-munksjo.showpad.com/share/mK0HxCgLgOU98L0q7n9cs

[40] S. M. V., Mathematical Theory of the Kinetics of the Coagulation of Colloidal Solutions, Z. Phys. Chem. 92 (1917) 129–168.
URL https://cir.nii.ac.jp/crid/1570854175868226816.bib?lang=en

[41] A. Vijaykumar, P. G. Bolhuis, P. R. Ten Wolde, The intrinsic rate constants in diffusion-influenced reactions, Faraday Discussions 195 (2016) 421–441. doi:10.1039/c6fd00104a.

[42] Y. Liu, L. Zhan, Z. Qin, J. Sackrison, J. C. Bischof, Ultrasensitive and Highly Specific Lateral Flow Assays for Point-of-Care Diagnosis, ACS Nano 15 (3) (2021) 3593–3611. doi:10.1021/acsnano.0c10035.